

Binary Segmentation of Malaria Parasites Using U-Net Segmentation Approach: A Case of Rwanda



Eugenia M. Akpo, Carine P. Mukamakuza, and Emmanuel Tuyishimire

Abstract Malaria is a significant health issue in Rwanda. Its accurate identification is essential for effective treatment. Traditional methods, such as microscopy, often face limitations in these contexts. This paper investigates how advanced machine learning techniques can address diagnostic challenges commonly encountered in resource-limited settings like Rwanda. A powerful deep learning framework known as U-Net was utilized in this study to identify different types of malaria. This method demonstrated the ability to accurately identify the disease at a highly detailed level, yielding promising results. The findings from this study could contribute to the development of computer-aided diagnostic tools specifically designed for regions with limited resources. These tools could assist healthcare professionals in decision-making processes and enhance patient outcomes.

Keywords Malaria diagnosis · U-Net architecture · Malaria parasite segmentation

1 Introduction

Malaria is a deadly disease that is typically present in tropical regions and spread by infected mosquito bites. Fever, headache, chills, nausea, vomiting, diarrhea, anemia, and respiratory distress are among the symptoms [1]. It can cause consequences like cerebral malaria, breathing issues, organ failure, anemia, and low blood sugar if left untreated. By avoiding mosquito bites, using pesticides, sleeping beneath nets, donning long pants and shirts, and using creams or sprays to repel mosquitoes, malaria can be avoided. Physical examination, symptoms, and blood tests are used to make the diagnosis. Depending on the patient's age and health status, several

E. M. Akpo (✉) · C. P. Mukamakuza
Carnegie Mellon University Africa, Kigali, Rwanda
e-mail: eakpo@andrew.cmu.edu

C. P. Mukamakuza
e-mail: cmukamak@andrew.cmu.edu

E. Tuyishimire
College of Science and Technology, University of Rwanda, Kigali, Rwanda

© The Author(s) 2024

X.-S. Yang et al. (eds.), *Proceedings of Ninth International Congress on Information and Communication Technology*, Lecture Notes in Networks and Systems 1011, https://doi.org/10.1007/978-981-97-4581-4_12

treatments may be available [1]. Plasmodium parasites can be categorized into five distinct species, namely *P. falciparum*, *P. vivax*, *P. ovale*, *P. knowlesi*, and *P. malariae*. Among these, *P. falciparum* and *P. vivax* are the most virulent and account for most malaria cases [2].

Malaria is a severe disease, with 241 million infections and 627,000 deaths in 2020, with Africa having the highest number of cases and fatalities [3]. Commonwealth governments committed to eliminating malaria by 2030 [1]. There have been various studies on automating the process of malaria detection in various parts of the world. The common consensus is that using the Giemsa-stained specimen/blood sample observed under microscopic slides, known as light microscopy, is the gold standard for malaria detection [4–6]. This process can be time-consuming and is only accurate based on the skill of the operator or technician. It can also be challenging in resource-limited settings, thereby having rapid diagnostic tests as the next alternative [7].

This paper is a part of a broader study in which the authors explore and suggest a digital system for monitoring malaria [8]. The proposed system aims to streamline the process of data collection, delivery, aggregation, classification, treatment reporting, repository updates, and public information services. This could potentially improve the forecasting, management, and treatment of malaria [8]. As a step in the right direction and in an effort to enhance malaria control, [9] created a data management model. The authors examine existing data management models and propose a novel one that is specifically designed for Rwanda. The specific objective of the study discussed in this paper is to enhance malaria prediction and automate the process of diagnosing malaria.

For malaria parasite detection and segmentation, numerous studies have explored both options and have found various results. Previous research in the field has shown that machine learning and artificial intelligence methods have the potential to aid in malaria detection significantly. In a foundational paper [10], advanced image analysis software and machine learning approaches were leveraged to identify malaria, showcasing the pivotal role of modern information technologies in effective disease mitigation. These methods encompassed image processing, cell segmentation, parasite identification, and feature calculation, underscoring the diversity of approaches within this domain [10].

Furthermore, recent research efforts have explored alternative methods for malaria parasite detection. For instance, the work in [5] employed scaled YOLOv4 and YOLOv5 object identification models to classify malaria parasites, achieving notable accuracy rates of 83 and 78.5%. This result suggests the potential for these algorithms to assist medical practitioners in accurately identifying and predicting the malaria stage, a crucial aspect of disease management. While much research has primarily focused on detecting *Plasmodium falciparum*, given its prominence and lethality in sub-Saharan Africa as recognized by the WHO [1], promising strides have been made in diversifying the approaches.

Another promising study is [11], where the authors suggest an automated analytic method for employing quantitative phase pictures to identify *Plasmodium falciparum*-infected red blood cells at the trophozoite or schizont stage. Linear discriminant classification (LDC), logistic regression (LR), and K-nearest neighbor

classification (NNC) are some of the techniques employed. Regarding schizont-stage detection, LDC has the best accuracy (up to 99.7%), whereas NNC has marginally greater accuracy (99.5%). These are all various studies contributing to automating malaria diagnosis.

This work explores Semantic segmentation, specifically the U-Net architecture, to segment malaria plasmodium species in digital image data collected in African settings, specifically Rwanda. Semantic segmentation groups image regions or pixels belonging to the same object class. It provides a helpful solution for various applications, including colon crypt segmentation, tumor identification, localization of surgical instruments, road sign detection, and land use classification. Semantic segmentation offers a well-defined method based on object class semantics, unlike non-semantic segmentation, which clusters pixels based on general object properties [12]. This differentiation highlights its adaptability and usefulness in various contexts, particularly medicine, which helps with disease diagnostics and organ segmentation [12]. U-Net is a famous semantic segmentation architecture proposed by Priyanshu et al. [13]. It is a customized convolutional neural network made specially for the segmentation of biomedical images. With skip connections, it has a recognizable “U” shape with an encoding path for feature extraction and a decoding path for up-sampling and accurate localization. U-Net has gained significant traction in biomedical image analysis, providing precise segmentation findings and inspiring the creation of comparable image segmentation designs across various applications [13].

The choice of employing the U-Net architecture is well justified. The U-Net architecture’s proven success in biomedical image analysis, particularly in segmenting Plasmodium, makes it a suitable and promising approach to address the challenges in this domain. The U-Net architecture has become more well-known in the biomedical industry because of the requirement for precise segmentation. U-Net’s capacity to concurrently integrate low-level and high-level information makes it suitable for medical image segmentation. High-level information makes it possible to extract intricate patterns, whereas low-level information enhances accuracy [14]. Consider the work by Abraham [15] which applies U-Net to segment Plasmodium within thin blood smear images and showcases U-Net’s remarkable accuracy in this task. This study examines three loss functions—mean-squared error, binary cross-entropy, and Huber loss—revealing that the Huber loss function outperforms the others. Testing metrics for F1 score, positive predictive value (PPV), sensitivity (SE), and relative segmentation accuracy (RSA) are notably higher with the Huber loss function, measuring 0.9297, 0.9715, 0.8957, and 0.9096, respectively. This underscores the effectiveness of U-Net coupled with the Huber loss function in achieving precise Plasmodium segmentation in thin blood smear images.

Furthermore, U-Net’s adaptability to different color spaces and its consistently high accuracy rates across RGB, HSV, and GGB color spaces make it a compelling choice for malaria parasite segmentation as demonstrated in [16]. In the RGB, HSV, and GGB color spaces, respectively, the findings demonstrate astounding accuracy rates of 99.40%, 99.36%, and 99.47%, highlighting the suggested technique’s durability [16].

Despite the effectiveness of U-Net, a predominant gap lies in the dataset's composition, consisting primarily of thin images of malaria parasites. This limitation could hinder the generalizability of developed models to more diverse and complex scenarios using thicker blood smears or different image types. Also, there is a dearth of studies addressing the diverse species of malaria parasites. The prevailing focus on a single species or the lack of species-specific identification in the literature could undermine the models' effectiveness in handling multiple species scenarios. Addressing these gaps will not only enhance the comprehensiveness of the research but also lead to more robust and accurate solutions in the field of malaria parasite detection and segmentation.

The rest of this paper is structured as follows: The detection includes the description of the extensive datasets acquisition and the U-Net architecture covered in Sect. 2; the results and discussion are covered in Sect. 3 followed by the limitations and recommendations in Sect. 4, and the conclusions are covered in Sect. 5.

2 The Detection Method

2.1 Datasets, Annotation, and Preprocessing

The dataset consists of a comprehensive collection of microscopic images that capture four types of malaria parasites: *Plasmodium falciparum*, *Plasmodium malariae*, *Plasmodium ovale*, and *Plasmodium vivax*. These images were meticulously collected at the Rwanda Biomedical Centre (RBC) [17] using a specialized microscope setup. The setup involved Giemsa-stained slides examined under a microscope, equipped with a camera attached to the eyepiece and connected to a laptop as shown in Fig. 1 [9].

As the microscope was adjusted, snapshots (fields) of the slides were taken and stored for further analysis. The images captured thick and thin film smears, providing a diverse range of samples for study. Each image was carefully annotated using the VGG Image Annotator 2.0.12 to ensure accuracy in identifying infected areas. This tool allowed for precise delineation of infected areas using its polygon feature.

The dataset was strategically divided to facilitate practical training, validation, and testing of the proposed U-Net-based segmentation model on various *Plasmodium* infections. An 80% allocation was made for training, with the remaining 20% equally divided between validation and testing for each parasite species. This division ensures a comprehensive representation of each parasite species across different subsets. This dataset provides a robust foundation for studying malaria parasites and developing effective machine learning models for their identification and classification. The detailed split and total number of images is found in Table 1.

The annotated masks were resized to a uniform dimension of 256×256 pixels and fed into the U-Net architecture. This standardization of image size not only ensures uniformity in training and results but boosts computational efficiency by minimizing



Fig. 1 Camera mounted on microscope at RBC to collect digital images of microscopic slides

Table 1 Summary of data split for all parasites

Parasite	Total	Train	Validation	Test
PF	58	46	6	6
PM	139	111	14	14
PO	191	152	19	20
PV	114	91	11	12

Note Abbreviations used: *PF* Plasmodium falciparum, *PO* Plasmodium ovale, *PV* Plasmodium vivax, *PM* Plasmodium malariae

the time and memory required. This preprocessing step guarantees that the mask sizes are consistent for the segmentation model, enabling smooth integration of the annotated data into the training, validation, and testing stages.

The samples used in this study were collected from patients with high fever who sought consultation at healthcare facilities. Positive slides were subsequently collected by the Rwandan Biomedical Centre for further analysis, including our research. Sample collection is primarily conducted at healthcare facilities across Rwanda on a quarterly basis for quality control purposes. RBC holds the legal authority for quality control, research, and training within Rwanda. This justifies the ethics of our study.

2.2 U-Net Architecture

The U-Net is a convolutional neural network architecture designed specifically for biomedical image segmentation tasks. It was introduced in a paper titled “U-Net: Convolutional Networks for Biomedical Image Segmentation,” authored by Ronneberger et al. [13]. The architecture is notable for its distinctive U-shaped design, which includes a contracting path (down-sampling) and an expansive path (up-sampling).

- **Contracting Path (Down-sampling):** The contracting path is responsible for reducing the spatial dimensions of the input image while capturing hierarchical features. It achieves this through a series of convolutional layers designed to detect patterns and features at different scales. The contracting path involves a series of convolutional and max-pooling layers that gradually reduce the spatial dimensions of the input image while extracting hierarchical features.
- **Expansive path (Up-sampling):** On the other hand, the expansive path is responsible for recovering the spatial resolution of the segmented regions. It uses transposed convolutions (deconvolutions) to up-sample the feature maps obtained from the contracting path. This helps the network recreate the finer details of the segmented objects. Additionally, during the up-sampling process, the expansive path incorporates information from the contracting path. This is achieved through concatenation operations, where feature maps from the contracting path are combined with those from the expansive path. This information fusion ensures that the network has context and spatial information for accurate segmentation.

The beauty of the U-Net architecture lies in the synergy between these two paths. The contracting path learns to extract meaningful features and patterns from the input image, while the expansive path uses this information to generate precise segmentation masks. This U-shaped design allows the U-Net to excel at biomedical image segmentation tasks where accuracy and detail preservation are crucial, making it a popular choice for tasks like cell nucleus segmentation or detecting intricate structures within medical images. Inspired by [18, 19], the following U-Net approach in Fig. 2 is used for this study.

2.3 Training

This work conducts individual binary segmentation on all four parasite types, with the architectural focus on precisely segmenting objects of interest from images while adeptly addressing the unique challenges inherent in binary image segmentation tasks. The model’s training leverages the Adam optimizer with a learning rate set to $1e-4$ and employs binary cross-entropy loss. Alongside accuracy, the model’s efficacy is gauged through the mean Intersection over Union (IoU) metric, quantifying the overlap between the predicted and actual masks. The training phase encompasses model fitting to the training dataset using a batch size of 16 for 300 epochs.

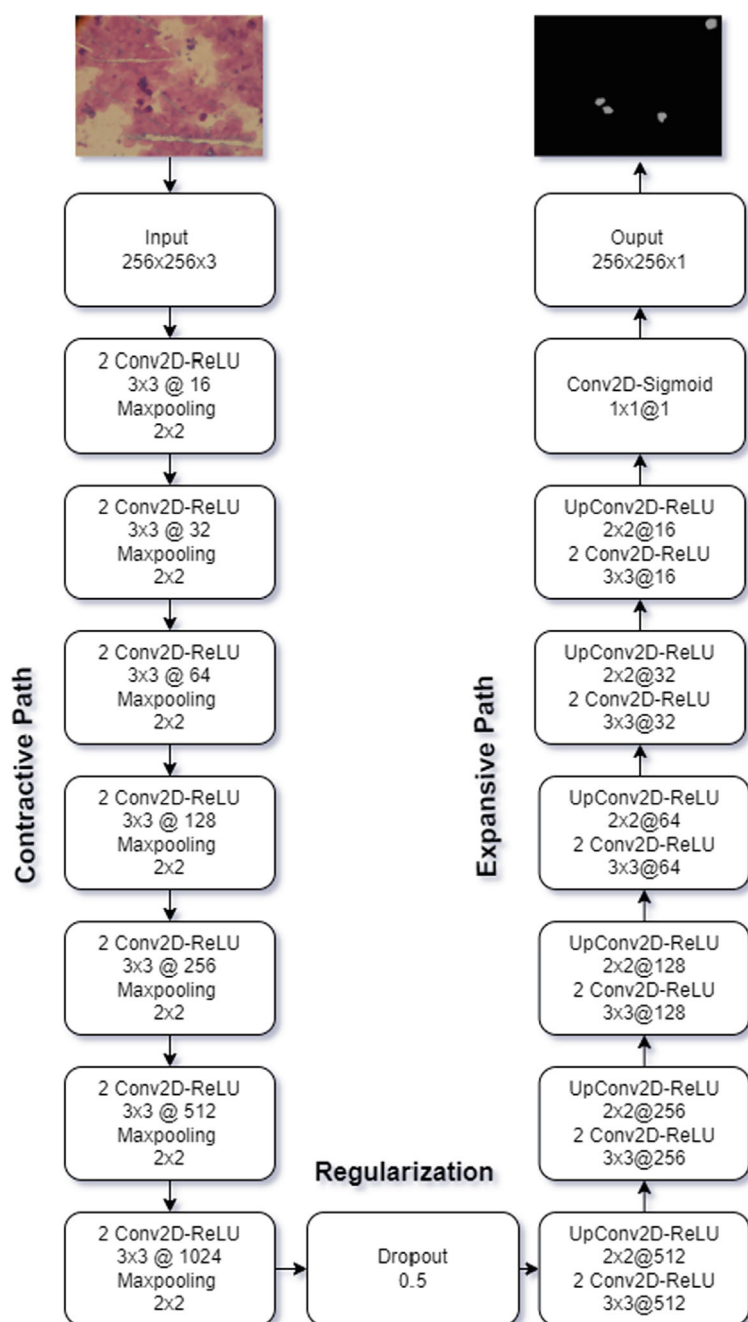


Fig. 2 U-Net architecture

- **Learning Rate (1e-2):** The learning rate controls how much to update the weight in the optimization algorithm. A smaller learning rate could lead to converging to the global minimum but might take more time to train, while a larger learning rate could speed up the training but risks overshooting the global minimum. In this case, a learning rate 1e-2 is chosen to balance convergence speed and assurance of not missing the global minimum [20].
- **Batch Size (16):** The batch size determines the number of samples propagated through the network simultaneously. A smaller batch size is chosen because it requires less memory to process, allows the model to start learning from data earlier, and provides a regular weight update, which can result in a robust model. The data size also accounts for why this figure was chosen. However, it might make the training process noisier and longer [20].
- **Number of Epochs (300):** The number of epochs is the number of times the entire dataset is passed forward and backward through the neural network. A higher number of epochs could lead to better performance until a certain point, after which the model might start overfitting. Therefore, 300 epochs are chosen to allow the model to learn complex patterns in the data without overfitting [21].

The model uses binary cross-entropy loss and Adam optimizer, which combines the advantages of two other extensions of stochastic gradient descent: AdaGrad and RMSProp. The mean Intersection over Union (IoU) metric is used for evaluating segmentation models by quantifying the overlap between the predicted and actual masks. Finally, precision, F_1 score, and recall metrics are explored via hyperparameter tuning to identify an optimal threshold yielding the highest F_1 score. The F_1 score is a performance metric commonly used in binary classification problems. The accuracy and comprehensiveness of the model are assessed using the harmonic mean of recall and precision. The F_1 score runs from 0 to 1, with 1 being the highest number that can be achieved [22, 23]. Unlike accuracy, it offers reliable findings for both balanced and unbalanced datasets.

3 Results and Discussion

Table 2 presents a concise overview of the outcomes obtained during the testing phases for all four parasite types. Figure 3 shows the training and validation loss of the model on the different *Plasmodium* species. Additionally, the ensuing figures in Fig. 4 offer visual representations of the model results on the four parasites, providing valuable insights into the project's performance.

The model achieved remarkable accuracy and low losses, yet there is potential for improvement when considering other evaluation metrics. Accuracy is a valuable metric when the classes are approximately equally distributed. It measures the proportion of correct predictions (true positives and negatives) among the total number of cases examined [24]. The F_1 score, combining precision and recall, provides a holistic view of the model's performance. *Plasmodium ovale* displays the highest

Table 2 Results of metrics on four parasites

Parasite	Loss	Accuracy	F_1 score	Precision	Recall
PF	0.0186	0.9955	0.0868	0.1175	0.0688
PM	0.0152	0.9969	0.5420	0.5282	0.5565
PO	0.0298	0.9882	0.6020	0.5444	0.6731
PV	0.0278	0.9840	0.5936	0.5365	0.6642

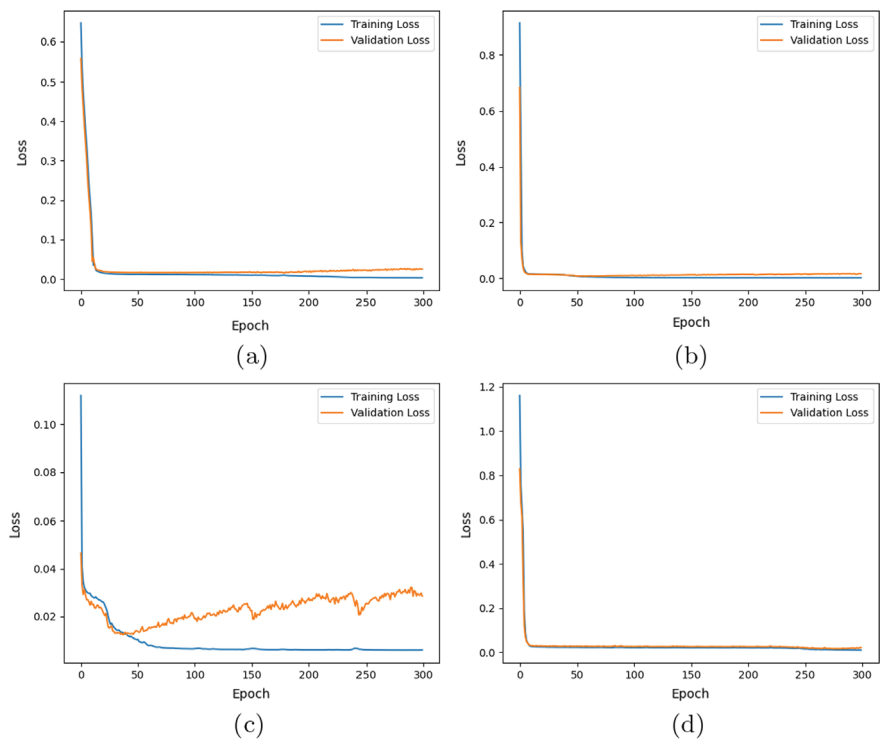


Fig. 3 Training result: **a** model on Plasmodium falciparum **b** model on Plasmodium malariae **c** model on Plasmodium ovale **d** model on Plasmodium vivax

F_1 score and recall among parasites, closely trailed by Plasmodium vivax and then Plasmodium malariae. In contrast, Plasmodium falciparum exhibits poorer performance, attributed to limited training data. Data augmentation was omitted to assess the model’s inherent learning. F_1 score, precision, and recall collectively showcase the segmentation’s efficacy. Plasmodium malariae exhibits peak accuracy, followed closely by falciparum, ovale, and vivax. F_1 scores align with training data, yielding results under 0.7. Visuals highlight accurate data detection, yet recall and precision at the optimal threshold are lacking.

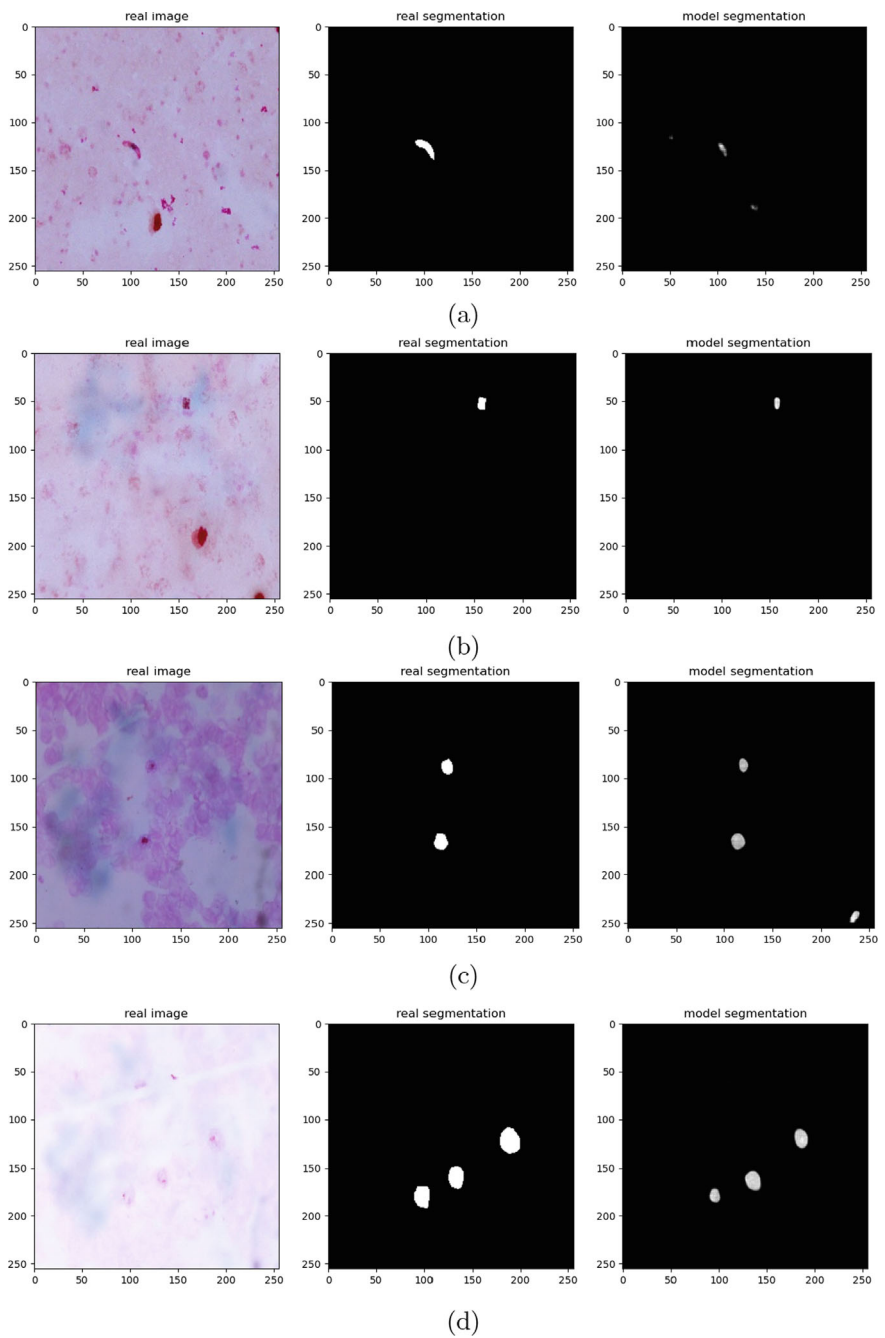


Fig. 4 Real image, ground truth, and model segmentation on the four parasites: **a** *Plasmodium falciparum* **b** *Plasmodium malariae* **c** *Plasmodium ovale* **d** *Plasmodium vivax*

Generally, the model accurately detects 99.6% of *Plasmodium falciparum*, 99.7% of *Plasmodium malariae*, 98.8% of *Plasmodium ovale*, and 98.4% of *Plasmodium vivax*. Despite strong accuracies, they might not fully depict effectiveness. The discrepancies between accuracies and other metrics reveal nuanced evaluation. In the study, while *Plasmodium malariae* exhibits peak accuracy, the F_1 -scores for all parasites are under 0.7. This discrepancy between accuracy and F_1 -score suggests that while the model is generally good at identifying the presence or absence of parasites (high accuracy), it may be less effective at correctly identifying positive cases (lower F_1 -score), particularly for classes with fewer instances in the training data [24].

4 Limitations and Recommendations

Effective diagnosis and treatment of malaria need efficient and precise segmentation of the parasites. As we explore the complexities of automatic segmentation using the U-Net architecture, a few crucial factors come into focus that may significantly impact the model's effectiveness and dependability. Three key limitations stand out and present opportunities for improvement.

One of the primary limitations of the current approach is the lack of a comprehensive dataset that encompasses the wide range of parasite variants, particularly for the *P. falciparum* parasite [25]. The model's effectiveness hinges on its ability to generalize across subtle variations. A larger dataset encompassing diverse parasite stages, morphologies, and image qualities can facilitate more effective learning. This enables the model to better address the complex challenges posed by various parasite species, fostering a comprehensive and adaptable solution. Data augmentation techniques can be employed to artificially expand the size and diversity of the training data, particularly when acquiring new data is challenging or expensive. This may be especially advantageous for the model's detection of *P. falciparum* parasites, which currently perform poorly due to a lack of training data [26].

In addition, the success of any segmentation model is inherently linked to the quality of its ground truth masks [27]. Investigating cutting-edge computer vision methods for producing these masks is essential to improving the precision of the F_1 -score and overall performance. Techniques such as instance segmentation, active contour modeling, and combining annotations from multiple perspectives should be utilized to achieve this [16]. Employing image processing techniques to eliminate or mitigate the impact of artifacts and white blood cells can further enhance the quality of ground truth annotations. Ground truth masks can be meticulously crafted by leveraging the strengths of these methods, effectively bridging the gap between manual annotation and automated detection. The outcome is a more streamlined and reliable training procedure that bolsters segmentation accuracy.

Furthermore, segmentation accuracy extends beyond data collection and model design. The choice of metrics and loss functions employed for evaluating model performance naturally influences the learning process and assessment accuracy. Exploring alternative solutions holds promise [28]. Investigating loss functions tailored to

the specifics of binary segmentation, such as Huber loss or dice loss, may lead to improved convergence and segmentation quality [15]. Additionally, incorporating metrics like the Matthews correlation coefficient (MCC) or the Jaccard index into the evaluation repertoire enables a more comprehensive assessment that considers various aspects of model performance.

Finally, one of the challenges faced is the inadequate training of laboratory technicians, resulting in poorly prepared malaria blood films. These substandard samples are often rejected, leading to delays in acquiring suitable specimens. Additionally, the inconsistent quality of stainings (reagents) can produce images with varying colorations. Experts must regularly check and validate reagents at endemic sites, further hindering the sample collection process.

By addressing the limitations identified and implementing the recommended improvements, the effectiveness and reliability of automatic segmentation of malaria parasites using the U-Net architecture can be significantly enhanced. This can lead to more accurate diagnoses and timely treatment decisions, improving patient outcomes and contributing to the fight against malaria.

5 Conclusion

The study reported accuracy levels of 99.6% for *Plasmodium falciparum*, 99.7% for *Plasmodium malariae*, 98.8% for *Plasmodium ovale*, and 98.4% for *Plasmodium vivax*, indicating a significant improvement in the accuracy of malaria diagnosis. Despite these impressive figures, there is potential for further improvement when considering other evaluation metrics such as the F_1 score, precision, and recall. The performance for *Plasmodium falciparum* was lower due to insufficient training data, highlighting the need for a comprehensive dataset for effective learning. The quality of ground truth masks and the choice of metrics and loss functions also significantly influence the model's success.

To extend this work, more data could be collected, advanced computer vision methods could be explored for each parasite, and other methods of segmentation such as MaskRCNN could be significantly explored. By implementing these steps, it is hoped that the model's performance can be enhanced, leading to more efficient and precise diagnosis and treatment of malaria. This study substantially contributes to malaria parasite detection and segmentation and identifies critical areas for future improvement. There are plans to implement automated malaria diagnosis in collaboration with the Rwandan Biomedical Centre (RBC), our most important stakeholder. This constitutes a part of the investigative phase, with the hope of transitioning to the deployment and testing phase with enhanced outcomes.

References

1. Commonwealth leaders take action in response to the Kigali Summit's call for bold commitments towards ending Malaria and Neglected Tropical Diseases (NTDs) | RBM Partnership to End Malaria. <https://endmalaria.org/news/commonwealth-leaders-take-action-response-kigali-summit%E2%80%99s-call-bold-commitments-towards-ending>
2. Shewajo FA, Fante KA (2023) Tile-based microscopic image processing for malaria screening using a deep learning approach. *BMC Med Imaging* 23(1):39
3. Fact sheet about malaria. <https://www.who.int/news-room/fact-sheets/detail/malaria>
4. Iqbal J, Hira P, Al-Ali F, Khalid N, Sher A (2003) Modified Giemsa staining for rapid diagnosis of Malaria infection. *Med Principles Pract* 12(3):156–159
5. Krishnadas P, Chadaga K, Sampathila N, Rao S, Prabhu S (2022) Classification of Malaria using object detection models. *Informatics* 9(4):76. <https://doi.org/10.3390/informatics9040076>, <https://www.mdpi.com/2227-9709/9/4/76>. Number: 4 Publisher: Multidisciplinary Digital Publishing Institute
6. Shambhu S, Koundal D, Das P, Hoang VT, Tran-Trung K, Turabieh H (2022) Computational methods for automated analysis of Malaria parasite using blood smear images: recent advances. *Comput Intell Neurosci* 2022:3626,726. <https://doi.org/10.1155/2022/3626726>, <https://www.ncbi.nlm.nih.gov/pmc/articles/PMC9017520/>
7. Kigozi RN, Bwanika J, Goodwin E, Thomas P, Bukoma P, Nabyonga P, Isabirye F, Oboth P, Kyoziira C, Niang M, Belay K, Sebikaari G, Tibenderana JK, Gudoi SS (2021) Determinants of malaria testing at health facilities: the case of Uganda. *Malaria J* 20(1):456
8. Mukamakuza CP, Tuyishimire E, Mbituyumuremyi A, Brown TX, Iradukunda D, Phuti O, Happiness RM (2022) A dependable digital system model for Malaria monitoring. preprint, *Mathematics and Computer Science*. <https://doi.org/10.20944/preprints202207.0461.v1>
9. Mary HR, Mukamakuza CP, Tuyishimire E (2023) A data management model for Malaria control: a case of Rwanda. In: 2023 IEEE AFRICON, pp 1–6. <https://doi.org/10.1109/AFRICON55910.2023.10293671>. ISSN: 2153-0033
10. Poostchi M, Silamut K, Maude RJ, Jaeger S, Thoma G (2018) Image analysis and machine learning for detecting malaria. *Transl Res* 194:36–55. <https://doi.org/10.1016/j.trsl.2017.12.004>. <https://www.sciencedirect.com/science/article/pii/S193152441730333X>
11. Park HS, Rinehart MT, Walzer KA, Chi JTA, Wax A (2016) Automated detection of *P. falciparum* using machine learning algorithms with quantitative phase images of unstained cells. *PLoS ONE* 11(9):e0163,045. <https://doi.org/10.1371/journal.pone.0163045>, <https://www.ncbi.nlm.nih.gov/pmc/articles/PMC5026369/>
12. Thoma M (2016) A survey of semantic segmentation. <https://arxiv.org/abs/1602.06541>. Publisher: arXiv Version Number: 2
13. Ronneberger O, Fischer P, Brox T (2015) U-Net: convolutional networks for biomedical image segmentation. <https://doi.org/10.48550/ARXIV.1505.04597>. Publisher: arXiv Version Number: 1
14. Liu X, Song L, Liu S, Zhang Y (2021) A review of deep-learning-based medical image segmentation methods. *Sustainability* 13(3):1224
15. Abraham JB (2019) Malaria parasite segmentation using U-Net: Comparative study of loss functions. *Commun Sci Technol* 4(2):57–62. <https://doi.org/10.21924/cst.4.2.2019.128>. <https://cst.kipmi.or.id/journal/article/view/128>
16. Nautre A, Nugroho HA, Frannita EL, Nurfauzi R (2020) Detection of Malaria Parasites in thin red blood smear using a segmentation approach with U-Net. In: 2020 3rd International conference on biomedical engineering (IBIOMED), pp 55–59. <https://doi.org/10.1109/IBIOMED50285.2020.9487603>
17. Welcome to RBC. <https://www.rbc.gov.rw/index.php?id=188>
18. Finalproject. <https://kaggle.com/code/alirezatohidi226/finalproject>
19. View of Malaria parasite segmentation using U-Net: comparative study of loss functions. <https://cst.kipmi.or.id/journal/article/view/128/60>

20. Priyanshu A, Naidu R, Mireshghallah F, Malekzadeh M (2021) Efficient hyperparameter optimization for differentially private deep learning. <http://arxiv.org/abs/2108.03888>, [ArXiv:2108.03888](https://doi.org/10.1007/978-3-642-35289-8_5) [cs]
21. Prechelt L (2012) Early stopping—but when? In: Montavon G, Orr GB, Müller KR (eds) Neural networks: tricks of the trade: second edition, lecture notes in computer science. Springer, Berlin, Heidelberg, pp. 53–67. https://doi.org/10.1007/978-3-642-35289-8_5
22. Hand DJ, Christen P, Kirielle NF (2020) An interpretable transformation of the F-measure. <https://doi.org/10.48550/ARXIV.2008.00103>. Publisher: arXiv Version Number: 3
23. Lipton ZC, Elkan C, Narayanaswamy B (2014) Thresholding classifiers to maximize F1 score. <https://doi.org/10.48550/ARXIV.1402.1892>. Publisher: arXiv Version Number: 2
24. Grandini M, Bagli E, Visani G (2020) Metrics for multi-class classification: an overview. <http://arxiv.org/abs/2008.05756>. [ArXiv:2008.05756](https://doi.org/10.48550/ARXIV.2008.05756) [cs, stat]
25. Su Z, Li W, Ma Z, Gao R (2022) An improved U-Net method for the semantic segmentation of remote sensing images. *Appl Intell* 52(3):3276–3288
26. Shorten C, Khoshgoftaar TM (2019) A survey on image data augmentation for Deep Learning. *J Big Data* 6(1):60
27. Malladi SRSP, Ram S, Rodriguez JJ (2018) A ground-truth fusion method for image segmentation evaluation. In: 2018 IEEE southwest symposium on image analysis and interpretation (SSIAI). IEEE, Las Vegas, NV, pp 137–140. <https://doi.org/10.1109/SSIAI.2018.8470317>
28. Wang Q, Ma Y, Zhao K, Tian Y (2022) A comprehensive survey of loss functions in machine learning. *Annals Data Sci* 9(2):187–212

Open Access This chapter is licensed under the terms of the Creative Commons Attribution 4.0 International License (<http://creativecommons.org/licenses/by/4.0/>), which permits use, sharing, adaptation, distribution and reproduction in any medium or format, as long as you give appropriate credit to the original author(s) and the source, provide a link to the Creative Commons license and indicate if changes were made.

The images or other third party material in this chapter are included in the chapter's Creative Commons license, unless indicated otherwise in a credit line to the material. If material is not included in the chapter's Creative Commons license and your intended use is not permitted by statutory regulation or exceeds the permitted use, you will need to obtain permission directly from the copyright holder.

